INVESTIGATION OF THE Cu-Co-Fe NANOSTRUCTURATED FILMS DEPOSITED BY THERMIONIC VACUUM ARC TECHNOLOGY

V. CIUPINĂ[a,b,d], D. ILIE[b*], R. MANU[b*], I. PRIOTEASA[b], I. JEPU[c], L. PETRĂŞESCU[b], P. DINCĂ[c], E. VASILE[e]

[a]*Department of Physics, "Ovidius" University of Constanta, Mamaia Ave., No. 124, 900527, Constanta, Romania,*
[b]*Faculty of Physics, The University of Bucharest, Atomistilor St., No. 405, PO Box MG-11, RO – 077125, Magurele, Ilfov, Romania,*
[c]*National Institute for Laser, Plasma and Radiation Physics, Atomistilor St., No. 409C, PO Box MG-36, 077125, Magurele, Ilfov, Romania,*
[d]*Academy of Romanian Scientists, Splaiul Independentei St, No. 54, 050094, Bucharest, Romania,*
[e]*Politehnica University of Bucharest, Splaiul Independenţei St, No. 313, RO-060042, Bucharest, Romania*

The main purpose of this paper is to investigate the morphology, chemical composition and magnetoresistive properties of Cu-Co-Fe thin films. These multilayers nanostructures were deposited on glass substrates. In this respect we used the Thermionic Vacuum Arc (TVA) method, wich assure a high purity of the obtined structures, provided by high vacuum pressure inside the coating chamber. Characterisation of the multilayer film in terms of the microstructure and elemental composition was provided using electron microscopy techniques (TEM and SEM), Energy Dispersive X-ray Spectroscopy (EDXS) and X-ray Diffraction Technique. Electrical measurements reveal that thin films have magnetoresistive properties. Magnetic properties were investgated by Magneto-Optic Kerr Effect (MOKE).

1. Introduction

Thin films have relevant applications in magnetic sensor technology, computer read/write heads and microelectromechanical systems MEMS. A magnetic field sensor based on GMR effect can directly detect a magnetic field and any changes in its intensity. It means that a variety of magnetic sensors can be used to detect parameters such as displacement, torque, position, current and many others. In order to synthesize nanostructured thin films, magnetic and nonmagnetic materials can be used. Magnetoresistive effect was obtained for Cu-Fe-Co thin films [1-8]. Cu was used for the nonmagnetic matrix, and for the magnetic matrix both Co and Fe were used alternatively.

2. Experimental system, techniques and approximations

Cu-Co-Fe films are deposited using TVA method [9-12] inside a vacuum chamber where two electron beams were emitted by two cathodes (TVA guns) and then they were accelerated by a high anodic voltage. The electron beams heat up and evaporates the anode material (Cu, Co and Fe) and assure their deposition on the glass substrates. The first gun evaporates copper from a crucible, and the second one alternately cobalt and iron from two different crucibles. Consequently, in vacuum, a steady state density of the metal vapours appears in the inter-electrode gap.

Corresponding authors: raducumanu@gmail.com

The value of the equivalent pressure of the metal vapours depends mainly on the power of the accelerated electron beam from the cathode. At further increase of the applied high voltage, suddenly a bright discharge appears in the inter-electrode space in the vapours of the anode material, with a simultaneous decrease of the voltage drop over the electrodes and with a significant increase of the current.

The thin films contain 16 layers (totalizing 160 nm), structured in 4 sets of 4 successive layers of Cu, Co, Cu and Fe. The thickness of the Cu, Co and Fe layers was 10 nm each. After deposition, some samples were thermally-treated at a temperature of 300 ^{0}C for 60 minutes. Unheated samples are labeled F_1, F_2, F_3 and thermally-treated samples are labeled F_4, F_5, F_6.

3. Experimental results and discussions

The elemental composition of the samples was established using X-ray Diffraction Techniques [13]. By indexing X-ray diffractogram, obtained for all samples, it was identified chemical composition and Miller indices for crystalline phases of copper, cobalt and iron, as shown in Fig. 1 and Fig. 2.
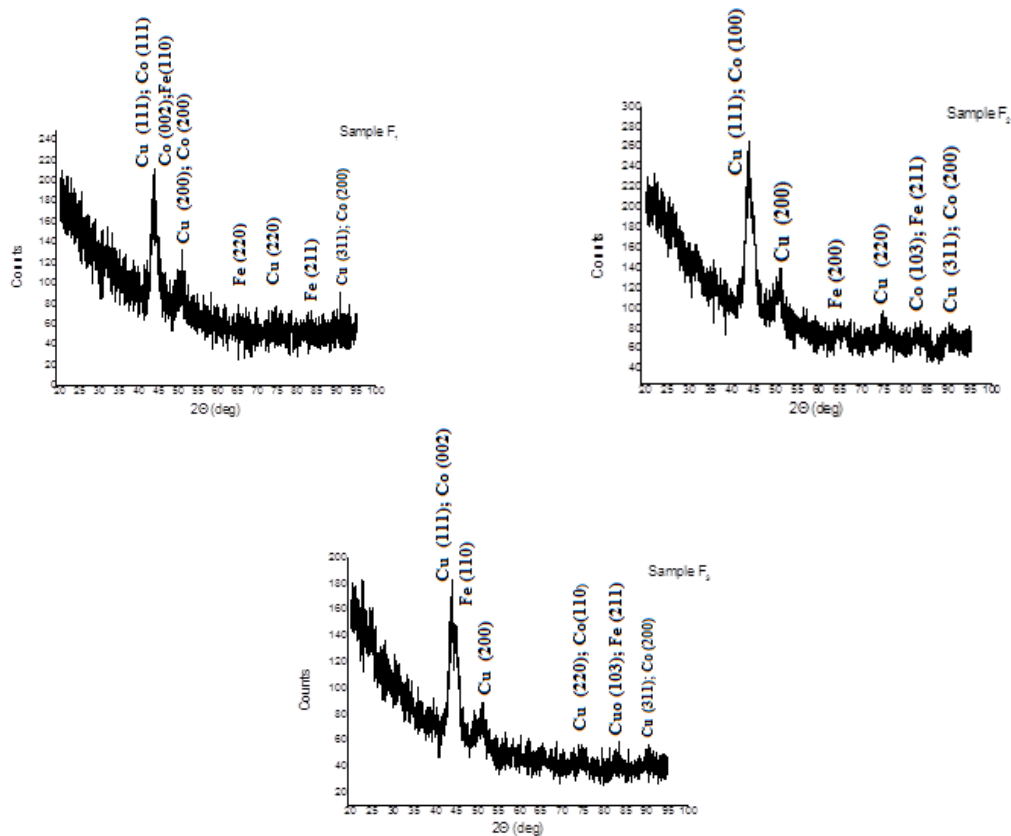

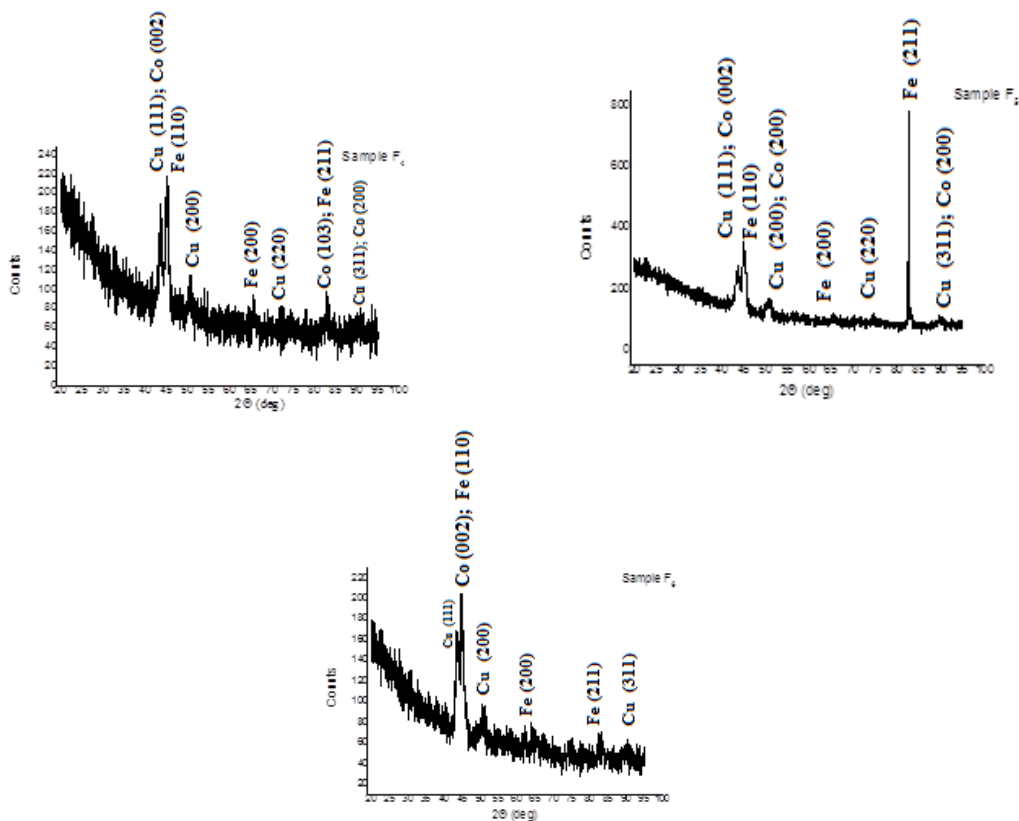Fig. 1. X-ray diffractograms corresponding to the unheated samples F_1, F_2 and F_3

Fig. 2. X-ray diffractograms corresponding to the thermally-treated samples F_4, F_5 and F_6

The aspect of the surface and the thickness of Cu-Co-Fe film were investigated using Scanning Electron Microscopy (SEM) technique. All the SEM images were obtained with secondary electrons – SEI. In order to obtain cross-sectional images, the samples were immersed in liquid nitrogen then they were fractured and examined. In Fig. 3.(a) is presented a cross-section through sample F_1, at a magnification of 200,000 times and confirms that the size of the film is about 157.4 nm. Fig. 3.(b) shows an image of the same sample at a magnification of 1,000000 times.
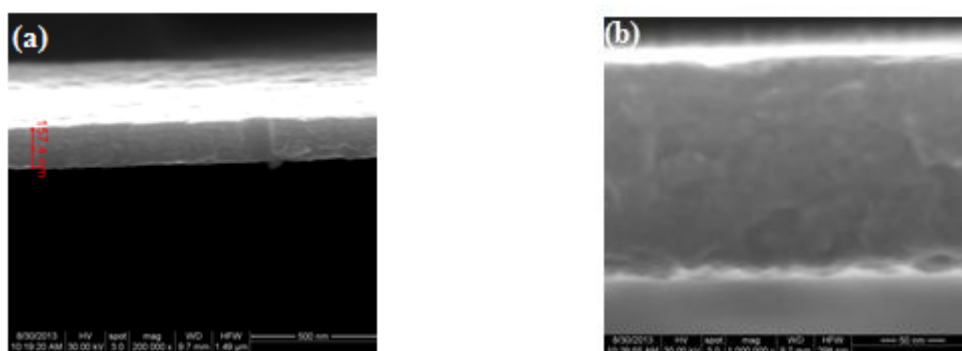

Fig. 3. (a) SEM image of the sample F_1 at a magnification of 200,000 times;
(b) SEM image of the sample F_1 at a magnification of 1,00000 times

The Energy Dispersive X-ray Spectroscopy (EDXS) technique allows the correlation between the microstructural characteristics and chemical composition of the sample. The SEM image of the sample F_1 is shown in Fig. 4(a) at a magnification of 60,000 times. Figure 4(b)

highlights EDX spectrum of the this sample (the diagram was represented using SEM technique). The EDXS detectors revealed the presence of the elements used to obtain thin film (Cu, Co, Fe) and other foreign elements such as: Mg , Al , Si, Ca, O, due to the glass substrate.
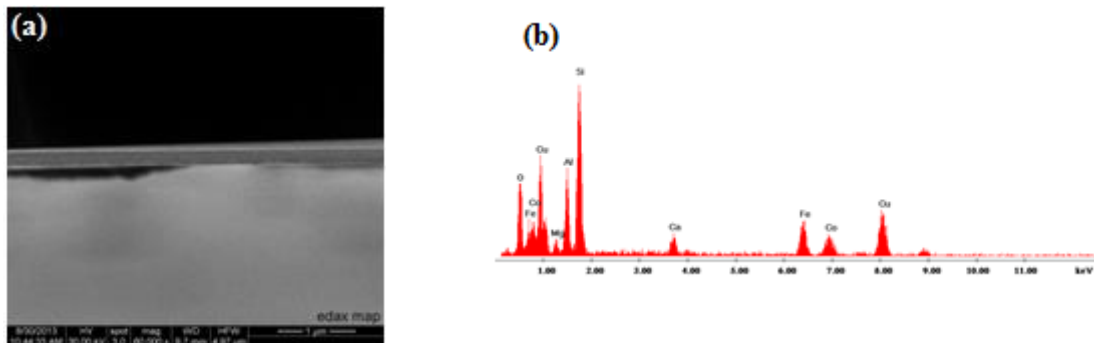

Fig.4. (a) SEM image of the sample F_1 (Cu-Co-Fe) on the glass substrate at a magnification of 60,000 times; (b) EDX spectrum corresponding to the same sample

Morphology and structure of the Cu-Co-Fe thin films were also analyzed using TEM techniques. Fig. 5 presents BF-TEM images obtained for the sample section F_1.
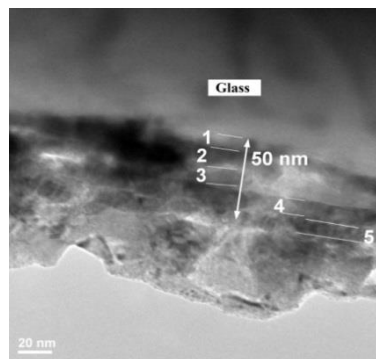

Fig. 5. BF-TEM image obtained on the sample F_1 (1-Cu;2-Co; 3-Cu; 4-Fe; 5-Cu)

Fig. 6 exposes HRTEM images of the sample F_1. Interplanar distances were measured for two layers within the film. For the lower layer, the interplanar distance corresponding to the Miller indices family (111) was measured indicating the presence of Face-Centered Cubic crystalline phase for copper. The interplanar distance of the top layer corresponds to the Miller indices family (110) which highlights the existence of the Body-Centered Cubic crystalline phase of iron. The thickness of this Fe layer is 10 nm.
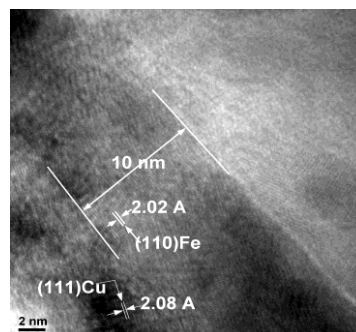

Fig. 6. HRTEM images obtained for sample F_1

Fig.7 reveals TEM image of sampleF$_4$ which highlights the presence of crystallites with diameters up to 9 nm.
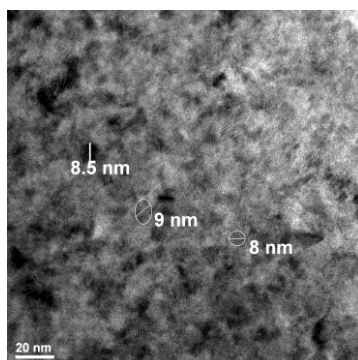

Fig. 7. TEM image obtained for sample F$_4$

In order to perform magnetoresistance measurements, ohmic contacts were attached to the samples.

Measurements were performed in two cases: when no magnetic field is applied, and in the case where the sample is placed in a magnetic field perpendicular to the surface of the sample [14], [15]. The sample resistance R_x was obtained comparing the voltage drop on the sample with the voltage drop on a series standard resistance in a constant current mode. Magnetoresistance is calculated using relation,

$$MR(\%) = (\Delta R_x / R_{x0}) \times 100\%, \tag{1}$$

here, $\Delta R_x = R_x - R_{x0}$, R_x being the resistance of the sample in magnetic field and R_{x0} the resistance of the sample in zero magnetic field. The magnetoresistance MR was measured for several values of temperature, as it shown in Table 1.

Table1. Experimental data obtained by magnetoresistance measurements

Unheated sample (F$_2$)									
B(T)	0.91					1.03			
T(K)	300	310	320	330	340	300	310	320	330	340
MR(%)	-8	-3.3	-5	-11	-10	-12	-3.9	-12	-20	-13

Thermally-trated sample (F$_5$)								
B(T)	0.90				1.01			
T(K)	300	310	320	330	300	310	320	330
MR(%)	-13	-26	-2	-5	-15	-35	-5	-4

Magnetoresistance of the samples depends on the external magnetic field at different temperatures, according to the diagrams from (Fig. 8). It can be seen that maximum value of magnetoresistance for unheated sample is -20% at 330K, in the presence of external magnetic field of 1.03T. The magnetoresistance of thermally-trated sample reaches a maximum of -35% at 310K, for external magnetic field of 1.01T.
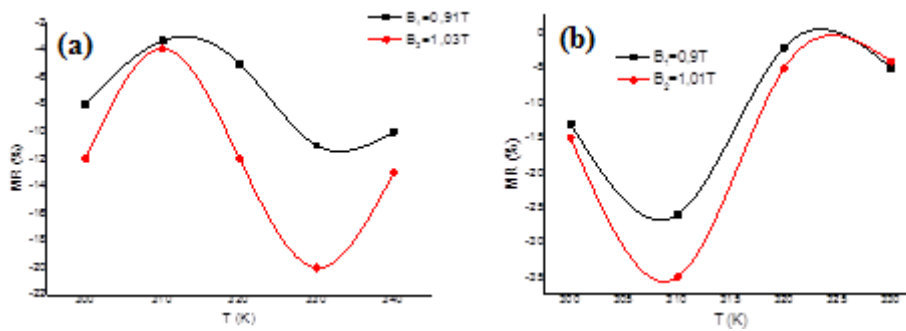
810

Fig. 8. (a) Magnetoresistance depending on temperature for unheated sample F₂;
(b) Magnetoresistance depending on temperature for thermally-treated sample F₅

In order to emphasize the magnetic properties, the Cu-Co-Fe thin films were analyzed in terms of Magneto-Optic Kerr Effect (MOKE). For thin films the values of the Kerr rotations were used depending on the external magnetic field, for the angles of 0^0, 45^0, 90, 135^0 and 180^0. Fig. 9 and Fig. 10 illustrate the MOKE signal for samples F_1, F_2, F_3 (unheated) and F_4, F_5, F_6 (thermally-treated), respectively.
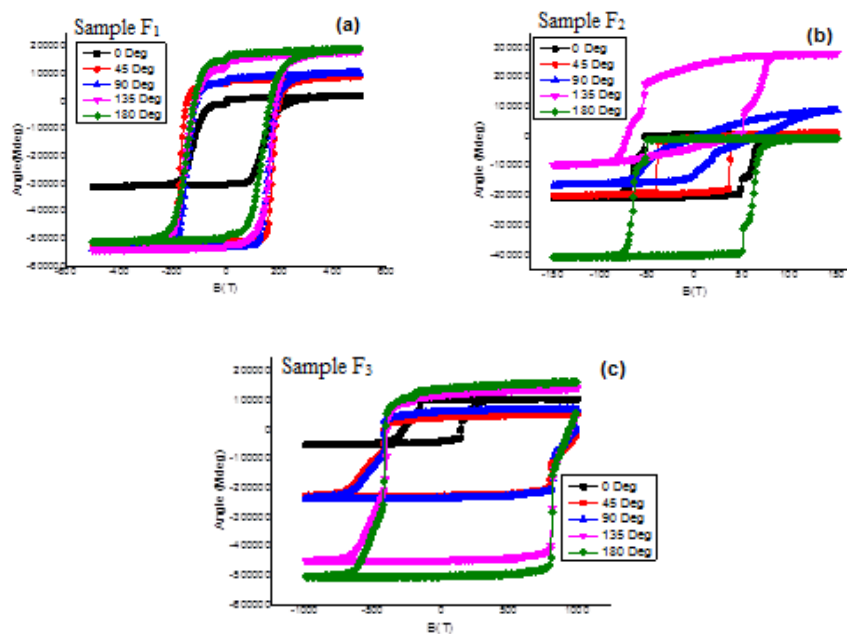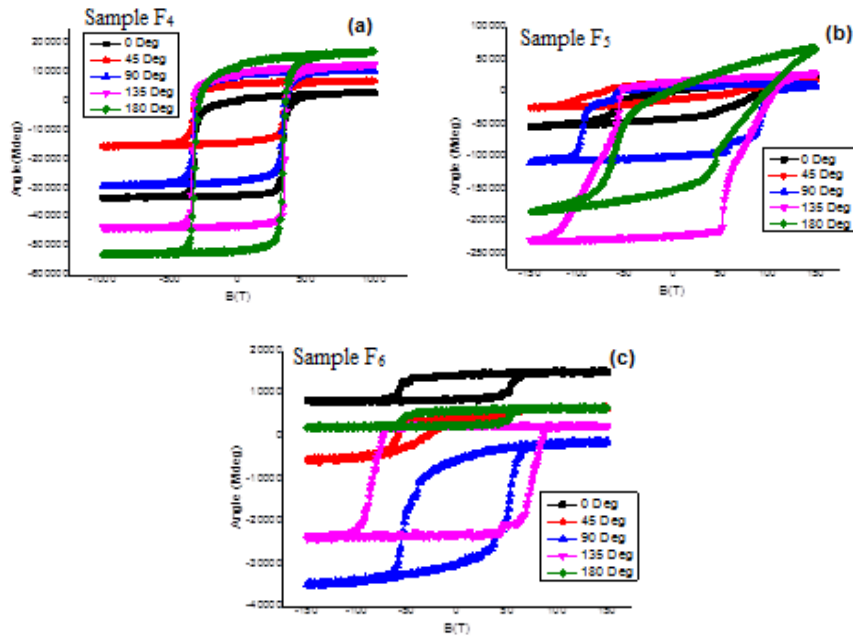

Fig. 9. Kerr rotation for sample F₁, F₂, F₃ (unheated)

Fig. 10. Kerr rotation for sample F_4, F_5, F_6 (thermally-treated)

The remanence values ratios depending on the rotation angle of the sample relative to the orientation of the magnetic field, were extracted and graphically represented (Fig. 11) for all samples.
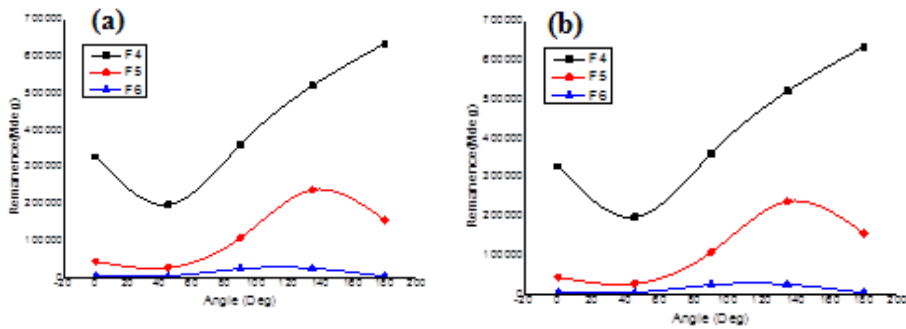

Fig. 11. The remanence value for the Kerr rotation corresponding to samples:
(a) F_1, F_2, F_3 (unheated), (b) F_4, F_5, F_6 (thermally-treated)

The ratio of the remanent magnetization and the saturation magnetization for Kerr rotation corresponding to all samples is represented in Fig. 12.
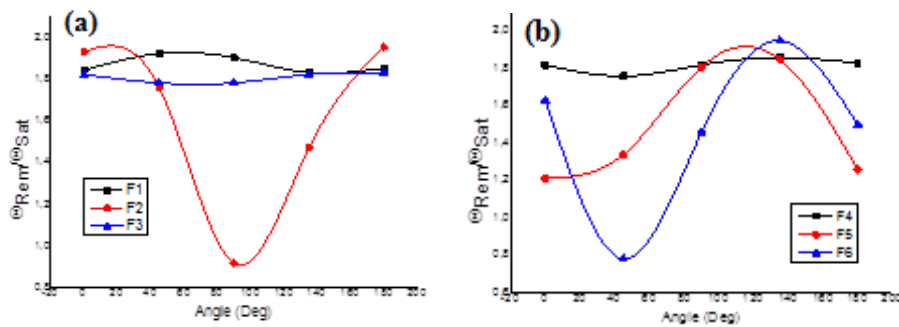

Fig. 12. The ratio of the remanent magnetization and saturation magnetization for Kerr rotation corresponding to samples: (a) F_1, F_2, F_3 (unheated), (b) F_4, F_5, F_6 (thermally-treated)

4. Conclusions

The aim of this study is to characterize thin multilayer Cu-Co-Fe films presenting high magnetoresistive effect. The method used to synthesize thin films was Thermoionic Vacuum Arc (TVA), which allowed us to create films of a high purity. X-ray diffraction identified the presence of the crystalline phases as follows: Face-Centered Cubic for Copper, Hexagonal for Cobalt and Body-Centered Cubic for Iron.

The morphology and structure of the thin films were analyzed using electron microscopy techniques (Transmission Electron and Scanning Electron Microscopy) which reveal that thin films consist in many crystallites forming a morphologically homogeneous film. The GMR effect was obtained, the maximum value of magnetoresistance was, for thermally-treated sample, -35% at 310K when the external magnetic field value was 1.01T. GMR effect measurements were performed in the CIP arrangement (current in plane). MOKE measurements confirme the ferromagnetic properties of thes multylaier structures.

References

[1] I. Jepu, C. Porosnicu, C. P. Lungu, I. Mustată, C. Luculescu, V. Kuncser, G. Iacobescu, A. Marin, V. Ciupina, Surface and Coatings Technology **240,** 344 (2014).
[2] C. P. Lungu, I. Mustata, G. Musa, V. Zaroschi, A. M. Lungu and K. Iwasaki, Vacuum, No. 2-3, 127 (2004).
[3] V. Kuncser, M. Valeanu, G.Schinteie, G. Filoti, I. Mustata, C. P. Lungu, A. Anghel, H. Chiriac, R. Vladoiu, J. Bartolome, Journal of magnetism and Magnetic Materials **320**(14), 226 (2008).
[4] M. Faris , M. EL Harfaoui, A. Qachaou, J. Ben Youssef, H. Le Gall, D.M. Mtalsi, M.J. Condensed Matter, **3**(1), p. 94-97 (2000).
[5] V. Stancu, C. Dragoi, V. Kuncser, G. Schinteie, L. Trupina, E. Vasile, L. Pintilie, Thin Solid Films **519**(19), 6269 (2011).
[6] F. Wang, T. Zhao, Z. D. Zhang, M. G. Wang, D. K. Xiong, X. M. Jin, D. Y. Geng, X. G. Zhao, W. Liu, M. H. Yu, F. R. de Boer, J. Phys. Condens. Matter **12**(11), 2525 (2000).
[7] Wu-Shou Zhang, Bo-Zang Li, Xiangdong Zhang, Yun Li, Journal of Applied Physics   No. 10, 71 (1998)
[8] V. Raghavendra Reddy, O. Crisan, Ajay Gupta, A. Banerjee, V. Kuncser, Thin Solid Films **520**(6), 2184 (2012).
[9] D. Ilie, D. Rasleanu, V. Ionescu, M. Mocanu, M.G. Muresean, I.M. Oancea-Stanescu, V. Ciupina, G. Prodan, E. Vasile, I. Must, V. Zaroschi, C.P. Lungu, J. Optoelectron. Adv. M. **12**(4), 839 (2010).
[10] M. Lungu, I. Tiseanu, C. Dobrea, C. Porosnicu, I. Jepu and JET-EUROfusion Contributors, Romanian Journal of Physics **60**(3-4), 560 (2015).
[11] C.P. Lungu, C. Porosnicu, I. Jepu, M. Lungu, A. Marcu, C. Luculescu, C. Ticos, A. Marin, C.E.A. Grigorescu, Vacuum, 110, p. 207-212, (2014)
[12] I. Jepu, C. Porosnicu, I. Mustata, C.P. Lungu, V. Kuncser, F. Miculescu, Romanian Reports in Physics **62**(4), 771 (2010).

[13] Umut Sarac, M. Celalettin Baykul, Journal of Materials Science, Materials in electronics, **25**(6), 2554 (2014).

[14] I. Jepu, C. Porosnicu, I. Mustata, C.P. Lungu, V. Kuncser, M. Osiac, G. Iacobescu, V. Ionescu, T. Tudor; Romanian Report in Physics **63**(3), 804 (2011).

[15] A. Anghel, C.P. Lungu, I. Mustata, V. Zaroschi, A.M. Lungu, I. Barbu, M. Badulescu, O. Pompilian, G. Schinteie, D. Predoi, V. Kuncser, G. Filoti, N. Apetroaei; Czech. J. Phys. **56**(2), 16 (2006).